DFT simulations and Raman spectroscopy properties of Capsaicin

Q. S. Martins*, , and D. L. L. Oliveira

Departamento de Física, Fundação Universidade Federal de Rondônia - UNIR, Ji-Paraná - RO, Brazil.
e-mail: quesle.martins@unir.br
orcid: 0000-0002-1315-2164

Received 16 May 2025; accepted 5 November 2025

A theoretical study of capsaicin was conducted using density functional theory (DFT) with the B3LYP and CAM-B3LYP functionals, combined with the 6-31G(d), 6-311+G(d,p), LanL2DZ, and CC-pVDZ basis sets. The study analyzed theoretical vibrational modes, Raman spectra, conformational energies, and global minima in geometric optimization. Results indicate that the LanL2DZ basis set provides the lowest conformational energies and the fastest computation times, whereas 6-31G(d) yields higher EPM values in VEDA. The CAM-B3LYP functional, particularly when combined with advanced basis sets such as 6-311+G(d,p) and CC-pVDZ, yields more accurate electronic property predictions. Overall, CAM-B3LYP/6-311+G(d,p) offers the best compromise between computational efficiency and spectral accuracy, while B3LYP/CC-pVDZ remains suitable for preliminary analyses.

Keywords: Capsaicin; DFT calculations; Raman spectroscopy; conformational analysis.

DOI: https://doi.org/10.31349/RevMexFis.72.030503

1. Introduction

Capsaicin (CA) is the active compound found in red pepper, responsible for its pungent taste and the subject of extensive research since its initial identification in 1919. Its chemical structure was determined in 1923 [1] and was chemically synthesized in 1930 [2]. It is a selective neuropeptide-releasing agent for primary peripheral sensory neurons. Peppers of the *Capsicum* genus (family *Solanaceae*) are among the most widely consumed spices in the world. However, as a chemical irritant, CA creates a burning sensation in humans and other mammals upon contact with biological tissues [3].

Frequently used as an analgesic, CA is found in various formulations, including creams, liquids, and patches in different concentrations. It is also present in dietary supplements [3] and dental applications [4] and is commonly associated with anti-inflammatory properties [4, 5].

Recently, Sheng-Hong Liu *et al*. (2022) [6] used CA as the gold standard for identifying residual oils based on Raman spectroscopy [6, 7]. Tian *et al*. (2018) [7] applied the same technique to detect CA in gutter oil. While Liu (2017) [8] applied Raman spectroscopy to identify CA in illegal cooking oils. El Kaaby (2016) [9] analyzed the spectrum of CA extracted from different *Capsicum annuum L*. pepper explants using Fourier Transform Infrared Spectroscopy (FT-IR). Cinar (2023) [10] demonstrated a strong correlation between experimental and DFT (Density Functional Theory) calculations for CA molecules.

Studies based on Density Functional Theory (DFT) have been fundamental in advancing the understanding of the structural, electronic and spectroscopic properties of CA. GP Sheeja Mol (2024) [11] used the 6-311++G(d,p) basis set. Roman (2024) [12] performed theoretical calculations using the hybrid methods B3LYP/6-31G(d) and B3LYP/6-311++G(d,p). Cinar (2023) [10] and (2010) [13] applied the B3LYP functional combined with the 6-311++G(d,p) basis set. Di Zang (2023) [14] utilized DFT/B3LYP parameters in a study on CA. Siudem (2017) [15] employed the DFT method with the B3LYP functional and the 6-31G(d,p) basis set, along with others such as 6-311+G(d,p), 6-31+G(d,p), and CC-pVDZ, investigating different functionals. Mustafa (2016) [16] used the LanL2DZ (B3LYP) basis set for structural and spectroscopic calculations. Leela (2015) [17] applied the B3LYP/6-311++G(d,p) method. These calculations have allowed the optimization of molecular geometry and the identification of preferred conformations.

To establish an efficient comparative framework among common optimization methods, in this study CA was analyzed using DFT calculations with the B3LYP and CAM-B3LYP functionals in combination with the LanL2DZ, 6-31G(d), 6-311+G(d,p), and CC-pVDZ basis sets.

2. Materials and methods

2.1. Capsaicin structure

CA (trans-8-methyl-N-vanillyl-6-nonenamide) (Fig. 1) is a crystalline, lipophilic, colorless, and odorless alkaloid with the molecular formula $C_{18}H_{27}NO_3$ [18]. The structure of CA consists of a hydrophilic aromatic ring, an amide bond, and a hydrophobic side chain [19]. The CA molecule was optimized using the Gaussian G09 software with the DFT method to obtain Raman vibrational spectra and molecular conformation data.

2.2. Computational methods

Computational calculations were performed using the Gaussian 09 package, optimizing the structure and predicting the harmonic vibrational Raman and IR frequencies [20]. Func-

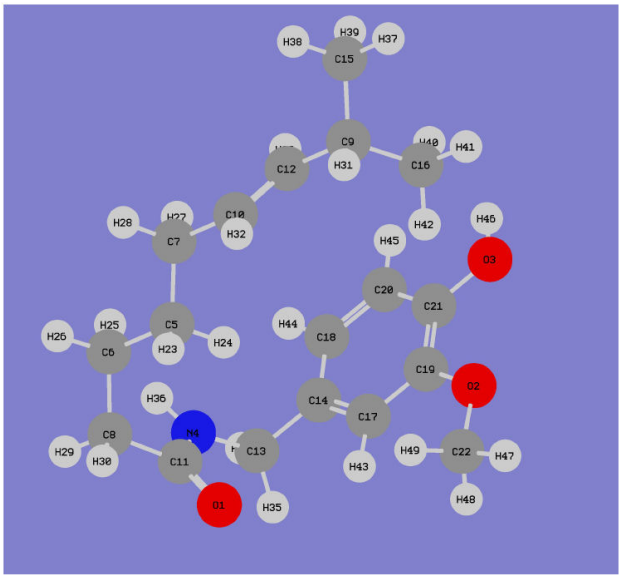

FIGURE 1. Molecular representation of CA. Carbon atoms are represented in gray, hydrogen in white, oxygen in red and nitrogen in blue. The functional structure of the molecule is identified, including the vanillyl group (on the right), the aliphatic chain and the central amide. The figure was generated based on optimized geometry via DFT calculations.

tional CAM-B3LYP/LanL2DZ, B3LYP/CC-pVDZ, and B3LYP/6-311+G(d,p) were employed. B3LYP is a three parameter function (B3) used for the Lee-Yang Parr (LYP) functional correlation exchange. The LYP correlation is a more cost-effective approach to calculating the molecular structure, vibrational frequencies, and energy of optimized structures [21–23]. CAM-B3LYP (A hybrid exchange-correlation functional using the Coulomb-attenuating method) is a tweak of B3LYP designed to improve the treatment of long-range interactions, especially in systems with excited states or long-range interactions (such as those involved in hydrogen bonding) [24].

Basis set: 6-311+G(d,p); Triple-polarized basis set for heavy atoms and polarized basis set for hydrogens, balancing accuracy and [25].6-31G(d); Double-polarized basis set and single difuse function. LanL2DZ uses pseudopotentials for heavy metals (mainly transition metals), useful in calculations of systems containing these metals [26]. CC-pVDZ; Correlated and polarized basis set, with good accuracy in DFT calculations for a wide range of molecules [27]. The choice of functionals and basis sets in this study was guided by the balance between computational cost and accuracy in describing the molecular properties of interest. The B3LYP functional, widely employed in studies of molecular structure and vibrational spectroscopy, provides consistent results with relatively low computational demand, making it suitable for comparative analyses of stability and vibrational frequencies. In addition, the CAM-B3LYP functional was considered due to its improved treatment of long-range exchange and excited-state interactions. Regarding the basis sets, different levels of flexibility were selected (6-31G(d), 6-311+G(d,p), LanL2DZ, and cc-pVDZ) to evaluate the sensitivity of the results to basis-set quality, ranging from more economical choices to those capable of describing electron correlation effects with higher accuracy.

3. Results and discussion

Figure 1 illustrates the optimized structure of the CA molecule obtained using G09. The VEDA software presented 48 stretching, 47 bending, 46 twisting, and also 75 CH stretching modes for CA the molecule.

Simulated Raman spectra (Figs. 2 and 3) of the CA molecule were obtained using three different functional combinations and basis sets. Figure 2, using the B3LYP functional combined with different basis sets (LanL2DZ, CC-pVDZ, 6-311+G(d,p), and 6-31G(d)), Raman peaks appear within similar wavenumber regions across all combinations, indicating that all methods adequately capture the primary vibrational modes of CA. The 6-311+G(d,p) basis set (magenta) exhibits more intense bands at low frequencies ($<$ 1000 cm^{-1}), suggesting a higher sensitivity of this basis to specific vibrational modes. Bands around 1600 cm^{-1}, characteristic of aromatic C=C stretching modes, show variable relative intensities, being more pronounced with the LanL2DZ and 6-311+G(d,p) basis sets. The 6-31G(d) basis set (yellow) tends to smooth the spectrum, resulting in lower peak resolution, reflecting its limitations in accurately describing vibrations of complex systems.

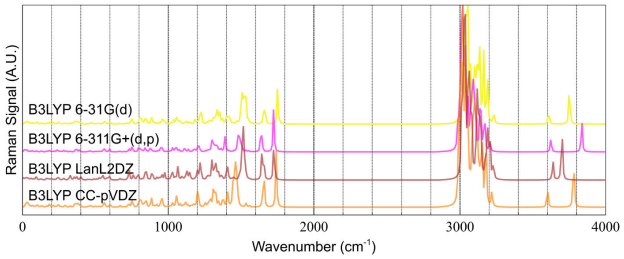

FIGURE 2. Simulated Raman spectra of the capsaicin molecule obtained from DFT calculations using the following combinations of functional and basis sets: B3LYP/LanL2DZ (brown), B3LYP/CC-pVDZ (orange), B3LYP/6-311+G(d,p) (magenta), and B3LYP/6-31G(d) (yellow).

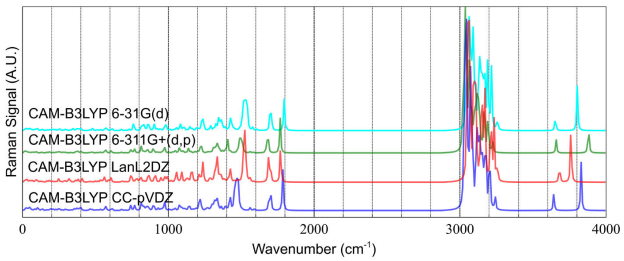

FIGURE 3. Simulated Raman spectra of the capsaicin molecule obtained from DFT calculations using the following combinations of functional and basis sets: CAM-B3LYP/LanL2DZ (red), CAM-B3LYP/CC-pVDZ (blue), CAM-B3LYP/6-311+G(d,p) (green) and CAM-B3LYP/6-31G(d) (cyan).

Figure 3, employing the CAM-B3LYP functionality with the same basis sets, the band positions remain similar in the same basis sets obtained from B3LYP. However, significant changes in intensity distribution indicates the influence of the exchange-correlation functional on polarizability. The CAM-B3LYP/6-311+G(d,p) spectrum (green) increased intensity and sharper features in the intermediate region (1000-1700 cm^{-1}), indicating an improved description of electronic transitions coupled with specific vibrations. These observations reveal that the CAM-B3LYP functional enhances spectral resolution and peak intensities in the 1000-1700 cm^{-1} region, which is critical for experimental comparative studies, as polar and aromatic group modes are well described. Regarding basis sets, more comprehensive sets like 6-311+G(d,p) provide better relative intensities and spectral detail, whereas simpler bases such as 6-31G(d) may lead to spectral information loss by underrepresenting complex vibrational modes.

The calculated spectra span a broad vibrational range (100-3700 cm^{-1}), encompassing characteristic modes of CA such as deformations, torsions, aromatic ring vibrations, C-C stretches, and C-H, O-H, and N-H stretching vibrations [10].

The CAM-B3LYP functional combined with the LanL2DZ basis set yields spectra with greater peak dispersion and variable intensities across the vibrational domain [16]. This method enhances bands around 1600-1700 cm^{-1}, typical of aromatic C=C stretching, as well as those in the 3000-3200 cm^{-1} region, assigned to C-H and O-H stretching [7, 10, 14]. The broader band distribution can be attributed to the sensitivity of CAM-B3LYP to long-range electronic effects, which amplify the number of vibrational modes simulated. In contrast, B3LYP combined with the CC-pVDZ basis set produces spectra with sharper, more defined peaks and relatively higher intensities, particularly in the 600-1800 cm^{-1} region. This approach improves spectral contrast, favoring Raman-active modes and providing an accurate description of aromatic ring vibrations along with amide and phenolic groups. The B3LYP/CC-pVDZ combination therefore represents an efficient balance between computational cost and accuracy, making it a widely validated choice for spectroscopic simulations of organic molecules.

In contrast, the spectrum generated with the B3LYP functional and the 6-311+G(d,p) basis set exhibits a smoother spectral profile, characterized by broader peaks and subtle frequency shifts relative to the other methods. Although the 6-311+G(d,p) basis set is robust and well suited for describing weak bonds and long-range interactions, it yields lower peak resolution, particularly in the high-frequency region ($> 3000\ cm^{-1}$). This suggests that, while advantageous for modeling complex interactions, this basis set may be less appropriate for capturing fine spectral details in high-resolution Raman studies [7, 14].

The spectral differences observed are intrinsically linked to the properties of the DFT functionals and basis sets employed. CAM-B3LYP, a long-range hybrid functional, incorporates exchange and correlation effects more extensively and is particularly sensitive to long-range electronic interactions, which accounts for the greater peak dispersion in its spectrum. B3LYP, by contrast, remains one of the most widely used functionals and provides a reliable description of electronic properties when combined with the CC-pVDZ basis set, which offers a favorable balance between accuracy and computational cost. The highly polarized and diffuse 6-311+G(d,p) basis set is effective for weak interactions but tends to reduce resolution under simplified vibrational approximations.

Comparing different DFT methods and basis sets is therefore essential for validating spectroscopic simulations against experimental data. Vibrational modes around 1600 cm^{-1} and $\approx 3200\ cm^{-1}$ are particularly informative for monitoring intermolecular interactions, including CA binding to biological receptors or solvation effects. Among the tested methods, B3LYP/CC-pVDZ delivers the best spectral resolution and is recommended for detailed spectroscopic studies, whereas CAM-B3LYP is more suitable for capturing a broader range of vibrational modes and complex electronic interactions, thus providing complementary insights for molecular investigations.

The vibrational modes observed between 700 and 1600 cm^{-1} (Fig. 1) are mainly associated with motions of the carbon chain and the benzene ring. C-C stretching modes are expected within 1400-1600 cm^{-1} [7], with specific bands detected at 1191, 1361, 1429, 1574, and 1606 cm^{-1}, assigned to symmetric stretching of υ(C-C), δ(C-H), υ(N=N), υ(C=C) in phenolic rings, and υ(C-N) groups [20,25]. Silverstein *et al*. [31] reported C-N stretching vibrations in the 1382-1266 cm^{-1} region for aromatic amines, while C-O stretching is usually found between 1260 and 1000 cm^{-1} [14]. In the present study, C-O stretching is instead assigned to the 1750-1800 cm^{-1} region. Additional assignments include: 1183 cm^{-1} (δCH_3 ring), 1219 cm^{-1} (δOH aromatic), 1312-1338 cm^{-1} (δCH), 1398 cm^{-1} (δCH), 1552 cm^{-1} (δNH), 1655-1665 cm^{-1} (υC=C phenyl), 1750 cm^{-1} (υC=C aliphatic), and 1769 cm^{-1} (υC=O amide). Vibrations corresponding to N-H stretching typically occur in the 3450-3250 cm^{-1} range. Above 3000 cm^{-1}, strong peaks at 3608 cm^{-1} (υNH) and 3751 cm^{-1} (υOH) are observed, the latter assigned to phenolic hydroxyl groups [7, 17].

In the high-frequency region, bands observed above 2800 cm^{-1} are mainly attributed to C-H stretching vibrations. Aliphatic C-H stretches from sp^3 hybridized carbons typically appear between 2850-2950 cm^{-1}, while sp^2 hybridized C-H bonds in aromatic and olefinic groups produce absorptions above 3000 cm^{-1}. In particular, features near or above 3050 cm^{-1} are characteristic of aromatic C-H stretching, associated with hydrogen atoms bonded to sp^2 carbons. These occur at slightly higher frequencies compared to the aliphatic stretches.

Overall, the results from Figs. 2 and 3 indicate that combinations involving CAM-B3LYP/6-311+G(d,p) are recommended for investigative protocols, as they produce spectra that better reproduce experimental features, including rel-

ative intensities and peak widths consistent with observations. However, smaller basis sets combined with conventional functionals (*e.g.,* B3LYP) remain useful for preliminary analyses, although they may overestimate certain bands and underestimate intensity transfers.

3.1. Parameters data for conformers

The general conformational data are presented in Table I. Table I results for B3LYP and CAM-B3LYP functionals with LanL2DZ, 6-31G(d), 6-311+G(d,p), and CC-pVDZ basis sets. The conformational values the lowest energy values for the LanL2DZ basis set (B3LYP) [15], with an energy of -982.445092 Hartree, compared to -982.070886 Hartree (CAM-B3LYP/6-31G(d)). Higher conformational values are observed for the 6-311+G(d,p) and CC-pVDZ basis sets in the B3LYP functional, respectively. The other sets show intermediate values.

The 6-31G(d) basis set demonstrated the highest efficiency in EPM parametrization, with values of 35.69 and 35.51 for the tested functionals. The LanL2DZ set the lowest EPM values in these respective cases.

Additionally, Table I reveals distinct values for polarizability. Basis sets with polarized and diffuse functions stand out for their higher polarizability values compared to the other sets. In this case, results obtained with the 6-311+G(d,p) basis set indicated values of 233.53 and 225.81. In the Raman effect, for example, the variation of the polarizability term is one of the factors responsible for activating vibrational modes present in the molecules [32].

The inclusion of diffuse (+) and polarization ("d" and "p") functions increases the accuracy of calculations for hydrogen and oxygen atoms, respectively. The CC-pVDZ basis set was optimized for computational efficiency by removing redundant functions and including polarization functions by default. These adjustments cause shifts in the bands above 3000 cm^{-1}, which can be observed in Fig. 2. The overestimated results are expected, as the calculations assume electron density free from any external disturbances. Since Raman spectroscopy detects vibrations related to changes in electric polarizability, polar molecular groups tend to show little or no activation in Raman measurements [29, 30].

Figure 4 shows the conformational data. Y axis: Potential energy (in electron volts, eV), with very negative values

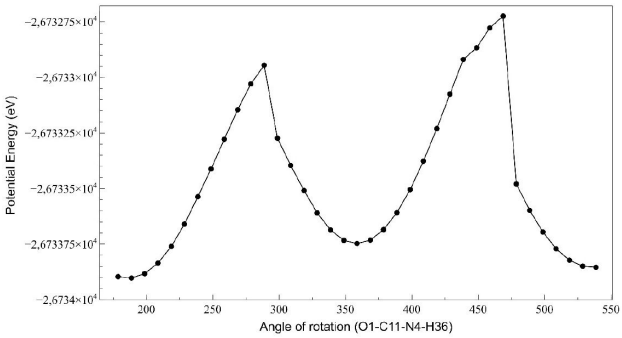

FIGURE 4. Conformational potential energy of the capsaicin molecule, obtained by DFT. Rotation angle (O1-C11-N4-36).

($\sim$ -26733 eV), indicating a highly stable molecule. X axis: Rotation angle (O1-C11-N4-H36), which implies a study of rotation around the C11-N4 bond, probably to understand rotational barriers and more stable conformations.

Figure 4 presented the conformational potential energy profile of the CA molecule obtained through DFT calculations for the dihedral rotation O1-C11-N4-H36. The curve three apparent minima; however, considering the periodic nature of the dihedral angle, a 360° rotation corresponds to the same molecular orientation. Therefore, only two distinct minima represent unique conformers, while the third reproduces the first due to rotational symmetry. A joint analysis with the data in Table II that the Scorpion conformer (Conformer 2) corresponds to the global minimum, exhibiting the lowest total energy and thus the most stable structure. The Compact and Extended conformers, on the other hand, correspond to local minima, characterized by slightly higher energies and representing metastable states along the rotation pathway.

Between these minima, energy peaks are observed that represent relatively low rotational barriers (on the order of 0.00005 eV), indicating significant conformational flexibility. This low barrier suggests that the molecule can easily interconvert between similar conformations at room temperature. This subtle variation is typical of rotations in single bonds, such as C-N in substituted amides or amines. Such conformational behavior may directly influence the interaction of CA with its biological targets, such as the TRPV1 receptor, affecting its biochemical and pharmacological activity [33, 34].

TABLE I. Computational data on energy, dipole, polarizability and EPM for different functionals and basis sets.

Functional	**B3LYP**				**CAM-B3LYP**			
Basis set	6-31G(d)	6-311+G(d,p)	LanL2DZ	CC-pVDZ	6-31G(d)	6-311+G(d,p)	LanL2DZ	CC-pVDZ
Energy (Hartree)	-982.5893	-982.8748	-982.4451	-982.6439	-982.0709	-982.3581	-981.9171	-982.1238
Dipole	3.3846	3.5465	4.2293	3.1307	3.5507	3.6116	4.4727	3.2541
Polarizability	202.000	233.530	202.600	213.287	196.511	225.809	196.500	207.281
EPM	35.69	34.610	33.44	35.339	35.51	33.973	33.55	35.193

Energy (Hartree): One Hartree is equal to 2625.5 kJ/mol, 627.5 kcal/mol, 27.211 eV, and 219474.6 cm^{-1}. The energy reported from a calculation is the energy required to separate the molecule into nuclei and electrons [36].

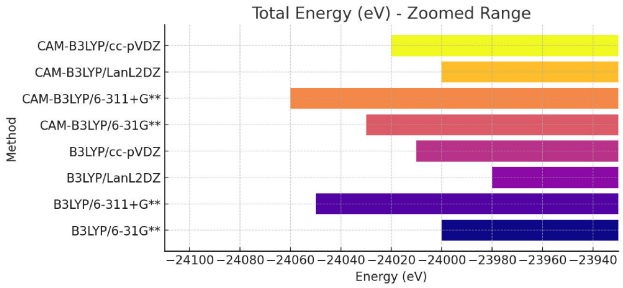

FIGURE 5. Total energy of capsaicin calculated using different DFT methods (Hartree to eV conversion). Lower values indicate greater stability.

Thus, the CA molecule reveals the presence of three distinct energy minima. The global minimum, which represents the most stable conformation, occurs around 340°, presenting the lowest potential energy value recorded ($\approx -2.6734 \times 10^4$ eV). In addition, two local minima are observed at approximately 200° and 520°, which indicate conformations that are also stable, but energetically less favored. The existence of these multiple minima suggests that CA can adopt different conformations in the equilibrium state, with preference for the conformation associated with the global minimum.

Table I presented computational data related to energy, dipole moment, polarizability, and the EPM parameter for different combinations of functionals (B3LYP and CAM-B3LYP) and basis sets (6-31G(d), 6-311+G(d,p), LanL2DZ, CC-pVDZ). The CAM-B3LYP functional yields slightly lower energies (Energy (Hartree)) than B3LYP, indicating greater energetic stability [35]. Figure 5 shows the energies obtained for the different parameters. The combination with the LanL2DZ basis set results in the lowest energy values for both functionals.

As seen from Fig. 5, the results show very similar total energies, with only minor relative differences compared to the absolute magnitude of approximately $-24,000$ eV. Long-range corrected functionals (CAM-B3LYP) yield slightly lower total energies than conventional B3LYP, indicating greater molecular stabilization in this case. The choice of basis set also influences the results, as more extended bases, such as 6-311+G(d,p), produce slightly more negative total energies than simpler ones, such as 6-31G(d,p), due to their greater flexibility in describing electronic orbitals. Although these differences are on the order of only a few tens of eV, they are significant when the aim is to compare methods or to evaluate molecular properties that depend on total energy. The dipole moment varies depending on the basis set, with the highest value observed for CAM-B3LYP with LanL2DZ (4.472728), suggesting greater charge separation (Fig. 6).

CAM-B3LYP generally provides higher dipole moment values compared to B3LYP. Polarizability values range from 196.5 to 233.53, with CAM-B3LYP and 6-311+G(d,p) yielding the highest value. In general, CAM-B3LYP exhibits greater polarizability than B3LYP, indicating a more flexible

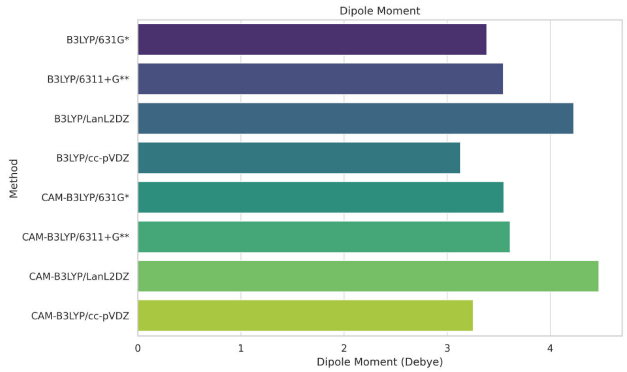

FIGURE 6. Comparison of dipole moments for capsaicin using various functionals and basis sets. Higher values suggest increased polarity.

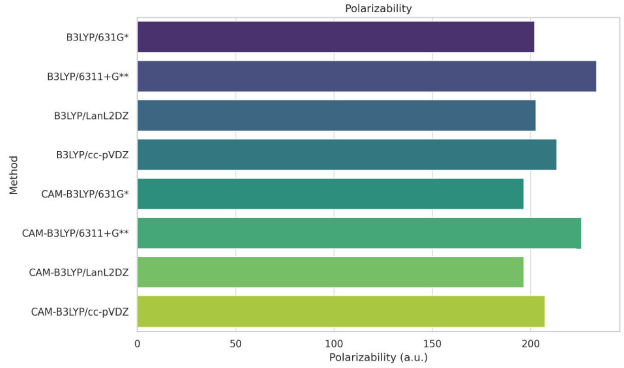

FIGURE 7. Average polarizability of capsaicin calculated with different DFT methods. Higher values indicate stronger Raman activity.

electronic response (Fig. 7). EPM values range from 33.44 to 35.69, with minor variations across different basis sets.

The highest EPM value (35.69) is obtained using B3LYP with 6-31G(d), while the lowest (33.55) is found with CAM-B3LYP and LanL2DZ (Fig. 8).

In Table I, the total energy values were originally obtained in Hartree units and converted to electron-volts (eV) using the relation 1 Hartree $\approx$ 27.2114 eV. The results show that the most stable configuration was obtained using the B3LYP/6-311+G(d,p) method, which presented the lowest energy: -982.878431 Hartree, corresponding to -26741.91 eV. In general, methods employing the CAM-B3LYP functional exhibited slightly less negative total energies, indicating less favorable energetic configurations compared to B3LYP. This behavior can be attributed to the nature of the CAM-B3LYP functional, which incorporates long-range corrections and tends to better represent electronic excitation phenomena, though it may slightly penalize ground-state energy.

Regarding the dipole moment, values ranged from 3.13 Debye (B3LYP/CC-pVDZ) to 4.47 Debye (CAM-B3LYP/LanL2DZ), revealing significant differences in the molecule's polarity depending on the method used. The highest value, obtained with CAM-B3LYP, suggests greater

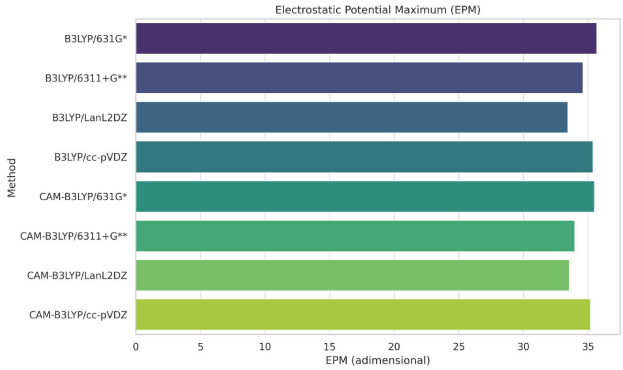

FIGURE 8. EPM values of capsaicin, representing vibrational optimization. Higher values suggest better geometry-vibration alignment.

charge separation and may indicate a more pronounced description of the electronic asymmetry of CA, which is relevant for studies of molecular interaction with polar environments such as solvents or biological receptors. This behavior is consistent with the purpose of the CAM-B3LYP functional, which typically generates more polarized electronic distributions. The average polarizability of the analyzed systems ranged from 196.5 a.u. to 233.5 a.u., with the B3LYP/6-311+G(d,p) method again standing out by presenting the highest polarizability (233.53 a.u.). This parameter is fundamental in Raman spectroscopy studies, because higher polarizability is associated with more intense vibrational modes and therefore simulated spectra with greater resolution and contrast. The combination of high polarizability and low total energy reinforces the suitability of B3LYP/6-311+G(d,p) for detailed vibrational descriptions.

The energy parameter maximum (EPM) is an adimensional value representing the percentage of structural optimization of the molecule in relation to the existing vibrational molecular groups. The values ranged from 33.44 to 35.69, reflecting minor variations in vibrational efficiency depending on the set of bases and the functional employed. The highest EPM was obtained with B3LYP/6-31G(d) (35.69), indicating a higher degree of agreement between the optimized geometry and the expected vibration modes, while the lowest value (33.44) was recorded with B3LYP/LanL2DZ. In general, methods that higher polarizability and lower total energy also higher EPM values, suggesting a correlation between geometric optimization and high-quality simulated spectroscopic properties.

Figure 9 showed different conformations 2, 19, and 37. The CA molecule exhibits significant conformational flexibility due to the presence of a long aliphatic chain, polar functional groups (such as amide, hydroxyl, and ether) and a substituted aromatic ring. Conformational analysis, performed through DFT calculations, allowed the identification of different local minima on the potential energy surface, representing conformations accessible to the molecule under various conditions.

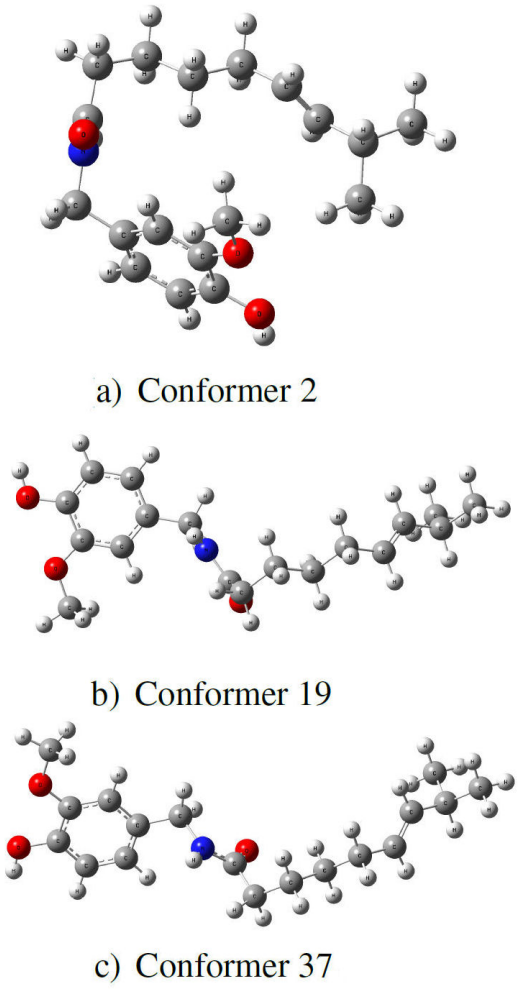

FIGURE 9. Representation of local minima and global minimum on the potential energy surface of the capsaicin molecule. a) Conformer 2 (“scorpion”) - more stable conformation, with possible intramolecular hydrogen bonding; b) Conformer 19 - interdicted structure with elongated side chain; c) Conformer 37 - compact structure with possible weak intramolecular interaction.

Conformation 2, known as the “scorpion conformer” [Fig. 9a)], features the molecule in a more folded state, with the amide group favorable to the formation of an intramolecular hydrogen bond, possibly involving a carbonyl and a nearby hydroxyl or amine group. This internal stabilizing interaction gives this conformation the lowest energy among those analyzed, characterizing it as the global minimum on the potential energy surface. However, its compactness may be entropically unfavorable in solution, especially in polar media, where the energetic gain from solvent interactions would be limited.

In conformation 19 [Fig. 9b)], the long side chain containing the vanillyl group is extended relative to the aromatic ring. The amide group adopts a relatively linear geometry. This structure favors dispersion interactions along the chain but may be associated with higher energy due to the reduced compactness of the molecule. In polar media, this conformation tends to be entropically disfavored because it extensively

exposes nonpolar groups to the solvent, thereby reducing its relative stability in such an environment.

In conformation 37 [Fig. 9c)], the side chain containing the amide group folds more, bringing the aromatic group closer to the end of the chain. This geometry suggests the possibility of weak intramolecular interactions, such as π-π or dipole-dipole interactions between molecular fragments. The relative compactness may make it more stable in nonpolar environments, as it reduces the exposure of polar groups to the solvent, optimizing the interaction with the medium.

3.2. Energetic comparison of the conformers

The energies obtained for the three conformations are presented in Table II associated with the O1-C11-N4-H36 dihedral rotation. It is noted that the most compact structure, which allows the formation of an intramolecular hydrogen bond (Conformer 2), exhibits the lowest total energy and is therefore the most stable conformer in the gas phase.

Conformation 2 ("scorpion") - Global minimum. This is the most energetically stable conformation, being 0.16 eV ($\approx$ 3.7 kcal/mol) more stable than Conformation 19. Its folded structure likely enables the formation of an intramolecular hydrogen bond (between NH and C=O or OH), making the molecule more compact [15]. This internal interaction reduces the total energy of the molecule, thus stabilizing the system. It also represents a typical structure for binding to biological receptors, as it presented a more accessible functional core [11].

Conformation 37. Approximately 0.05 eV ($\approx$1.2 kcal/mol) above the global minimum. It may represent a transition state or a viable conformation in solution. Although not the most compact, it may exhibit internal dipole-dipole interactions. Thermodynamically, it is a reasonably favored structure.

Conformation 19. The most expanded, with minimal intramolecular interaction. Around 0.16 eV ($\approx$3.7 kcal/mol) above the global minimum, which is a significant difference on a molecular scale. It may occur in systems with high rotational freedom (such as in the gas phase or at high temperatures), but it is less favored in biological or polar environments. Differences of up to 1 kcal/mol ($\approx$0.043 eV) still allow conformational co-existence (see, *e.g.*, Conf. 2 and 37), but above 3 kcal/mol (as in the case of 19), co-existence at equilibrium becomes significantly less likely. The fact that Conformation 2 is the global minimum suggests that it is the most prevalent under equilibrium conditions, especially in condensed phases (solution or membranes). In summary, the B3LYP/6-311+G(d,p) method demonstrates the best overall performance for the structural and spectroscopic description of CA, providing the lowest energy, the highest polarizability and an electronic profile consistent with high-quality simulated Raman spectra. However, CAM-B3LYP methods, although less energetically stable, stand out for their higher polarity and sensitivity to long-range electronic interactions, making them preferable for studies involving solvation, electronic excitation, or molecular coupling. The CA molecule presented several stable conformations associated with the O1-C11-N4-H36 dihedral rotation, with small energy barriers between them. This indicates that, under normal thermal conditions, it can adopt multiple similar geometries, which may influence its flexibility [37].

TABLE II. DFT-calculated energies of capsaicin conformers.

Conformer	Total Energy (eV)	Stability Classification
19 - Extended	-26733.74	Highest in energy
37 - Compact	-26733.85	Intermediate
2 - Scorpion (Global Minimum)	**-26733.90**	Most stable

4. Conclusions

Among the tested methodologies, the CAM-B3LYP functional combined with the 6-311+G(d,p) basis set exhibited superior performance in reproducing the experimental spectral features, offering an optimal balance between computational efficiency and accuracy. CAM-B3LYP yields the lowest conformational energies across all tested basis sets compared to B3LYP and provides improved molecular polarizability values. B3LYP spectra are largely comparable below 1800 cm^{-1}; however, the 6-31G(d) and LanL2DZ basis sets show shifts in C=O, N-H, and aliphatic O-H vibrations, respectively. Overall, CAM-B3LYP, particularly when paired with sophisticated basis sets such as 6-311+G(d,p) and CC-pVDZ, delivers more accurate electronic property values.

The choice of basis set significantly influences the dipole moment and polarizability, affecting the description of the molecule's electronic distribution. Conformational analysis indicates three main structures for CA: Conformation 2 ("scorpion"), the most stable due to an intramolecular hydrogen bond; Conformation 37, intermediate in stability, stabilized by dipole-dipole interactions in nonpolar environments; and Conformation 19, a more extended and less stable structure.

Acknowledgments

The authors acknowledge that PIBIC-CNPQ was financially supported by FAPERO (Grant Number 003/2024) and PROPESQ (Grant Number EDITAL No 003/2023/DPESQ/PROPESQ/UNIR). The Laboratório de Física Aplicada (LFA), research group Física Experimental e Aplicada (UNIR) and Estrutura da Matéria e Física Computacional, DAF/JP - UNIR.

1. E. K. Nelson and E. Dawson, The constitution of capsaicin, the pungent principle of capsicum. *J. Am. Chem. Soc.* **45** (1923) 2179, https://doi.org/10.1021/ja01662a023
2. E. Späth and S.F. Darling, Synthese des Capsaicins, *Ber. dtsch. Chem. Ges. A/B* **63**(1930) 737, https://doi.org/10.1002/cber.19300630331
3. National Center for Biotechnology Information. PubChem Compound Summary for CID 1548943, Capsaicin. PubChem, https://pubchem.ncbi.nlm.nih.gov/compound/Capsaicin
4. C. Kim *et al*., Capsaicin exhibits anti-inflammatory property by inhibiting IkB-a degradation in LPS-stimulated peritoneal macrophages, *Cellular Signalling* **15** (2003) 299, https://doi.org/10.1016/S0898-6568(02)00086-4
5. M. H. Yang, S. H. Jung, G. Sethi, and K. S. Ahn, Pleiotropic Pharmacological Actions of Capsazepine, a Synthetic Analogue of Capsaicin, against Various Cancers and Inflammatory Diseases, *Molecules*, **24** (2019) 995, https://doi.org/10.3390/molecules24050995
6. S. Liu *et al*., Label-free SERS strategy for rapid detection of capsaicin for identification of waste oils, *Talanta* **245** (2022) 123488, https://doi.org/10.1016/j.talanta.2022.123488
7. K. Tian *et al.*, Rapid identification of gutter oil by detecting the capsaicin using surface enhanced Raman spectroscopy. *J. Raman Spectrosc.* **49** (2018) 472, https://doi.org/10.1002/jrs.5306
8. Z. Liu, S. Yu, S. Xu, B. Zhao, and W. Xu, Ultrasensitive detection of capsaicin in oil for fast identification of illegal cooking oil by SERRS. *Acs Omega* **2** (2017) 8401, https://doi.org/10.1021/acsomega.7b01457
9. A. Ekhlas, N. A. H. Zahra, and A. A. Jenan, FT-IR Identification of Capsaicin from callus and seedling of chilli pepper plants Capsicum annuum L. in vitro, *Int. J. Multidiscip. Curr. Res.* **4** (2016) 1144, https://ijmcr.com/index.php/ijmcr/article/view/04.06.09/672
10. M. Çınar, B. Alim, Z. Alim, E. Şakar, Determination of the molecular structure and spectroscopic properties of capsaicin. *Rad. Phys. Chem.* **208** (2023) 110879, http://dx.doi.org/10.2139/ssrn.4292963
11. G. P. S. Mol, D. Aruldhas, I. H. Joe, S. Selvaraj, and A. G. Nadh, Modeling the structural and reactivity properties of capsaicin [(E)-N-[(4-hydroxy-3-methoxyphenyl)methyl]-8-methylnon-6-enamide] wavefunction-dependent properties, pharmacokinetics, in-silico analysis, and molecular dynamics simulation, *J. Mol. Struct.* **1304** (2024) 137591, https://doi.org/10.1016/j.molstruc.2024.137591
12. E. Romano *et al*., Identification of cholesterol in different media by using the FT-IR, FT-Raman and UV-visible spectra combined with DFT calculations, *J. Mol. Liq.* **403** (2024) 124879, https://doi.org/10.1016/j.molliq.2024.124879
13. M. Karabacak, M. Cinar, and M. Kurt, DFT based computational study on the molecular conformation, NMR chemical shifts and vibrational transitions for N-(2-methylphenyl) methanesulfonamide and N-(3-methylphenyl) methanesulfonamide, *J. Mol. Struct.* **968** (2010) 108, https://doi.org/10.1016/j.molstruc.2010.01.033
14. D. Zhang *et al*., SERS determination of hydroxy-α-sanshool in spicy hotpot seasoning: The strategy to restrain the interference of capsaicin and its mechanism, *Food Chem.* **413** (2023) 135644, https://doi.org/10.1016/j.foodchem.2023.135644
15. P. Siudem, K. Paradowska, J. Bukowicki, Conformational analysis of capsaicin using 13C, 15N MAS NMR, GIAO DFT and GA calculations, *J. Mol. Struct.* **1146** (2017) 773, https://doi.org/10.1016/j.molstruc.2017.05.142
16. M. T. Bilkan, Ş. Yurdakul, Z. Demircioğlu, O. BüyükgüngÃ¶r, Crystal structure, FT-IR, FT-Raman and DFT studies on a novel compound [C10H9N3]4AgNO3, *J. Organomet. Chem.* **805** (2016) 108, https://doi.org/10.1016/j.jorganchem.2016.01.014
17. J. S. P. P. Leela, R. Hemamalini, S. Muthu and A. A. Al-Saadi, Spectroscopic investigation (FTIR spectrum), NBO, HOMO-LUMO energies, NLO and thermodynamic properties of 8-Methyl-N-vanillyl-6-nonenamideby DFT methods, *Spectrochim. Acta A* **146** (2015) 177, https://doi.org/10.1016/j.saa.2015.03.027
18. M. D. L. Reyes-Escogido, E. G. Gonzalez-Mondragon, and E. Vazquez-Tzompantzi, Chemical and pharmacological aspects of Capsaicin, *Molecules* **16** (2011) 1253, https://doi.org/10.3390/molecules16021253
19. N. D. Kambaine, D. M. Shadrack, and S. A.H. Vuai, Conformations and stability of Capsaicin in bulk solvents: A molecular dynamics study, *J. Mol. Liq.* **345** (2022) 117794, https://doi.org/10.1016/j.molliq.2021.117794
20. M.J. Frisch *et al*., Gaussian 09, (2009).
21. A. D. Becke, Density-functional thermochemistry. III. The role of exact exchange, *J. Chem. Phys.* **98** (1993) 5648, https://doi.org/10.1063/1.464913.
22. C. Lee, W. Yang and R. G. Parr, Development of the Colle-Salvetti correlation-energy formula into a functional of the electron density, *Phys. Rev. B* **98** (1988) 785, https://doi.org/10.1103/PhysRevB.37.785.
23. X. Wu, S. Gao, J. S. Wang, H. Wang, Y. W. Huanga and Y. Zhaod, The surface-enhanced Raman spectra of aflatoxins: spectral analysis, density functional theory calculation, detection and differentiation, *Analyst* **137** (2012) 4226, https://doi.org/10.1039/C2AN35378D.
24. T. Yanai, D. P. Tew, and N. C. Handy, A new hybrid exchange-correlation functional using the Coulomb-attenuating method (CAM-B3LYP). *Chem. Phys. Lett.* **393** (2004) 51, https://doi.org/10.1016/j.cplett.2004.06.011
25. T. H. Dunning, Gaussian basis sets for use in correlated molecular calculations. I. The atoms boron through neon and hydrogen. *J. Chem. Phys.* **90** (1989) 1007, https://doi.org/10.1063/1.456153
26. P. J. Hay and W. R. Wadt, Ab initio effective core potentials for molecular calculations. Potentials for the transition metal atoms Sc to Hg. *J. Chem. Phys.* **82** (1985) 270, https://doi.org/10.1063/1.448547

27. K. A. Peterson and T. H. Dunning, Accuracy of correlation consistent basis sets for transition metal and first-row atoms. *J. Chem. Phys.* **117** (2002) 10548, https://doi.org/10.1063/1.1522883

28. M. H. Jamróz, Vibrational energy eistribution analysis (VEDA): Scopes and limitations, *Spectrochim. Acta A* **114** (2013) 220, https://doi.org/10.1016/j.saa.2013.05.096.

29. M. Meenu, E. A. Decker, and B. Xu, Application of vibrational spectroscopic techniques for determination of thermal degradation of frying oils and fats: a review. *Crit. Rev. Food Sci. Nutr.* **62** (2021) 5744, https://doi.org/10.1080/10408398.2021.1891520

30. J. A. Antunes *et al.,* Study on optical, electrochemical and thermal properties of the Meldrum acid 5-aminomethylene derivative, *Vib. Spectrosc.* **112** (2021) 103188, https://doi.org/10.1016/j.vibspec.2020.103188

31. R. M. Silverstein, G. C. Bassler and T. C. Morril Spectrometric Identification of Organic Compounds John Wiley, New York (1991).

32. C. A. Aguirre-Tellez, Q. S. Martins, and J. J. B. Ortega, Breve introducción al estudio Raman de partículas cargadas. *Rev. Ingenio* **20** (2023) 1, https://doi.org/10.22463/2011642X.3308

33. M. J. Caterina, M. A. Schumacher, M. Tominaga, T. A. Rosen, J. D. Levine and D. Julius, The Capsaicin receptor: a heat-activated ion channel in the pain pathway. *Nature* **389** (1997) 816, https://doi.org/10.1038/39807

34. D. H. Kwon, F. Zhang, Y. Suo, J. Bouvette, M. J. Borgnia, and S. Lee, Heat-dependent opening of TRPV1 in the presence of capsaicin. *Nat. Struct. Mol. Biol.* **28** (2021) 554, https://doi.org/10.1038/s41594-021-00616-3

35. A. Abkari, I. Chaabane, and K. Guidara, DFT (B3LYP/LanL2DZ and B3LYP/6-311G+**) comparative vibrational spectroscopic analysis of organic-inorganic compound bis(4-acetylanilinium) tetrachlorocuprate(II), *Physica E* **81** (2016) 136, https://doi.org/10.1016/j.physe.2016.03.010

36. V.K. Shen, D.W. Siderius, W.P. Krekelberg, and H.W. Hatch, Eds., NIST Standard Reference Simulation Website, NIST Standard Reference Database, National Institute of Standards and Technology, Gaithersburg MD, 20899, https://cccbdb.nist.gov/hartreex.asp

37. A. Alberti, V. Galasso, B. Kovač, A. Modelli, and F. Pichierri, Probing the Molecular and Electronic Structure of Capsaicin: A Spectroscopic and Quantum Mechanical Study, *J. Phys. Chem.* **112** (2008) 5700, https://doi.org/10.1021/jp801890g